Nickel Passivation in Acidic Chloride Solution Using Optical Second Harmonic Generation†

J. M. Frye, M. W. Schauer, M. J. Pellin,* and D. M. Gruen

Materials Science and Chemistry Divisions, Argonne National Laboratory, Argonne, Illinois 60439

C. A. Melendres

Materials Science and Chemical Technology Divisions, Argonne National Laboratory, Argonne, Illinois 60439

Received July 17, 1989

Optical second harmonic generation (SHG), originating at the interface of a highly polished nickel electrode in acidified chloride (0.1 M NaCl, 0.01 M HCl) solution, has been observed. Striking changes in the SHG intensity were observed accompanying the onset of passive film formation, with incident light at wavelengths (λ_0) of 1064 and 532 nm. Analyses of the SHG and cyclic voltammetry measurements lead to the following conclusions: (1) The existence of two peaks in the cyclic voltammogram (CV) at the $Ni^0 \rightarrow Ni^{2+}$ oxidation potential strongly suggests that passive film formation on polycrystalline nickel in this electrolyte is a two-step process. (2) Actual film formation is concurrent with the *second* (more anodic) peak in the CV, as is evidenced by the dramatic change in SHG (λ_0 = 1064 nm) observed at this potential. (3) The first peak appears to be due to dissolution. This is supported by the observation that the SHG (λ_0 = 532 nm) gradually drops in intensity at the potential when the first peak appears. These findings are consistent with the dissolution–precipitation mechanism of passive film formation initially proposed by Reddy, Rao, and Bockris. (4) SHG (λ_0 = 532 nm) is strongly influenced by surface roughening.

Introduction

Nickel is known to form a passive film that protects the metal from extensive corrosion. In an ongoing effort to better understand this film, nickel has been the subject of numerous experimental studies. The vast majority of the studies performed to date have investigated electrochemically induced film formation in basic solutions,[4-8] since such electrolytes are used in the nickel battery industry. Since the pertinent reaction in the nickel battery involves $Ni^{2+} \rightleftharpoons Ni^{3+}$ oxidation–reduction, previous studies have usually concentrated on the film that forms at potentials between those required for Ni^{2+} and Ni^{3+} formation, the so-called passive region, characterized by nondissolution of nickel. We have chosen, on the other hand, to study film formation in the much less studied chloride-containing acidic medium. Although films still form on nickel in such environments, they are not as protective against pitting–corrosion; it is well-known that chloride and other halide ions hinder passivation.[9-11] Previous work[1-3,12-15] still leaves unanswered many questions regarding the nature of the passivating film on nickel in acidic media. Controversy arises, in part, because of technique limitations. Illustrative examples are the ex situ nature of surface analytical techniques and the influence of surface roughening on ellipsometric data.[16]

To supplement existing techniques, we have employed optical second harmonic generation (SHG), a very sensitive probe of interfacial processes, to study film growth "in situ" in an electrochemical cell. In the electric dipole approximation, for centrosymmetric media, second harmonic light is generated only at the interface, where the symmetry is broken.[17,18] Intense light incident on the surface induces, in the medium, a polarization, P, which includes nonlinear as well as linear terms:

$$P = \chi^{(1)}:\mathbf{E} + \chi^{(2)}:\mathbf{EE} + \chi^{(3)}:\mathbf{EEE} + \ldots \quad (1)$$

$\mathbf{E}$ refers to the electric field vector of the incident radiation. $\chi^{(n)}$ is the nth order term in the nonlinear expansion of the dielectric constant of the medium and is usually a complex number. The imaginary part of $\chi^{(1)}$ is proportional to the absorption coefficient of the medium, and the first term on the right gives rise to linear absorption spectroscopy. SHG results from the next two terms. Specifically, if the incident radiation is at a single frequency ω, the polarization induced in the medium at twice the incident frequency gives rise to frequency-doubled light. If the frequency of the incident or second harmonic light corresponds to a transition frequency in the material at the interface, a large enhancement in SHG can occur due to resonance effects.[19,20] If, in addition, the surface is exposed to a large dc electric field, such as exists at the electrode–solution interface in an electrochemical cell, the

†Work performed under the auspices of the U.S. Department of Energy, BES-Materials Sciences, under contract W-31-109-ENG-38.

(1) Reddy, A. K. N.; Rao, M. G. B.; Bockris, J. O'M. *J. Chem. Phys.* **1965**, *42*, 2246.
(2) Bockris, J. O'M.; Reddy, A. K. N.; Rao, B. *J. Electrochem. Soc.* **1966**, *113*, 1133.
(3) Reddy, A. K. N.; Rao, B. *Can. J. Chem.* **1969**, *47*, 2687.
(4) Falk, S. U.; Salkind, A. J. *Alkaline Storage Batteries*; Wiley: New York, 1969.
(5) Briggs, G. W. D. *Chem. Soc. Spec. Period. Rep., Electrochemistry 4* **1979**, 33.
(6) Oliva, P.; Leonardi, J.; Laurent, J. F.; Delmas, C.; Braconnier, J. J.; Figlarz, M.; Fievet, F.; deGuibert, A. *J. Power Sources* **1982**, *8*, 229.
(7) Beden, B.; Bewick, A. *Electrochim. Acta* **1988**, *33*, 1695.
(8) Biwer, B. W.; Pellin, M. J.; Schauer, M. W.; Gruen, D. M. In preparation.
(9) Burstein, G. T.; Wright, G. A. *Electrochim. Acta* **1975**, *20*, 95.
(10) MacDougall, B. *J. Electrochem. Soc.* **1970**, *126*, 919.
(11) Hsu, Y. S.; Wu, J. K. *J. Mater. Sci. Lett.* **1987**, *6*, 1246.
(12) Chao, C. Y.; Szklarsha-Smialowska, Z.; MacDonald, D. D. *J. Electroanal. Chem.* **1982**, *131*, 289.
(13) Smith, R. J. Ph.D. Thesis, University of Florida, 1984.
(14) Hummel, R. E.; Smith, R. J.; Verink, Jr., E. D. *Corros. Sci.* **1987**, *27*, 803.
(15) Bosio, L.; Cortes, R.; Delichere, P.; Froment, M.; Joiret, S. *Surf. Interface Anal.* **1988**, *12*, 380.
(16) Smith, T.; Smith, P.; Mansfield, F. *J. Electrochem. Soc.* **1979**, *126*, 799.
(17) Bloembergen, N.; Chang, R. K.; Jha, S. S.; Lee, C. H. *Phys. Rev.* **1968**, *174*, 813.
(18) Guyot-Sionnest, P.; Chen, W.; Shen, Y. R. *Phys. Rev. B* **1986**, *33*, 8254.
(19) Heinz, T. F.; Chen, C. K.; Richard, D.; Shen, Y. R. *Phys. Rev. Lett.* **1982**, *48*, 478.
(20) Heuer, W.; Schröter, L.; Zacharias, H. *Chem. Phys. Lett.* **1987**, *135*, 299.

0897-4756/90/2802-0245$02.50/0

polarization at twice the incident frequency will include a term due to charging of the Helmholtz bilayer:[21-23]

$$P(2\omega) = \chi^{(2)}:\mathbf{E}(\omega)\ \mathbf{E}(\omega) + \chi^{(3)}:\mathbf{E}(\omega)\ \mathbf{E}(\omega)\ \mathbf{E}_{dc} \quad (2)$$

where $\chi^{(2)}$ is the lowest order nonlinear susceptibility tensor, $\chi^{(3)}$ is the next higher order nonlinear term, or hyperpolarizability tensor, and $\mathbf{E}_{dc}$ refers to the charge on the surface. Although $\chi^{(3)}$ is usually much smaller than $\chi^{(2)}$, large electric fields can give rise to SHG due to surface charging effects, of intensity comparable to that due to $\chi^{(2)}$.

In the experiments described herein, SHG, in conjunction with cyclic voltammetry, has been used to gain a better understanding of the mechanism of film formation on nickel in an acid chloride electrolyte.

Experimental Section

Details of the experimental apparatus have been described elsewhere.[8,24] Briefly, the working electrode consisted of a 2.0-mm-diameter polycrystalline nickel rod (99.9975% pure), sealed to a quartz sleeve with heat-shrinkable Teflon. The exposed end surface was ground with silicon carbide paper (600 and 1200 grit) and then polished with 1-μm diamond paste and 0.05-μm alumina (Buehler Products). The counterelectrode, also composed of high-purity nickel, was lightly sanded before each measurement with emery paper; all voltages cited herein are with respect to the saturated calomel electrode (SCE). Nanopure water was used in the acid chloride solution (0.01 M HCl/0.1 M NaCl), which was not deaerated.

In all cases, after the cell was assembled, the potential was slowly swept from the open-circuit voltage (typically -0.2 V_{SCE}) to -0.7 V_{SCE}, the starting voltage of our cyclic voltammogram (CV), in order to reduce the air-formed oxide. During the CV, the anodic switching potential was low enough ($+0.25$ V_{SCE}) to avoid excessive pitting of the electrode. If a second cycle was desired after the first cycle, the potential was slowly swept to ≈ -1 V_{SCE}, to ensure reduction of the electrochemically formed oxide. In all cases, the scans began at a potential no lower than -0.7 V_{SCE} to avoid hydrogen evolution, as the bubbles tend to scatter the incident beam.

Incident radiation was provided by a mode-locked Nd:YAG laser, Q-switched at 1 kHz. Typically, the pulse length was 100 ps, which enabled us to employ photon-counting techniques. This is a necessity if one wishes to observe SHG from metals with very small nonlinear susceptibilities, such as nickel and iron,[25] without damaging the surface. Either the fundamental (1064 nm) or frequency-doubled (532 nm) output of the laser was directed first through a phase retarder for polarization selection (p in these experiments) and then through a filter to remove any SHG originating from reflections from mirror surfaces. Finally, the laser beam was focused onto the polished electrode surface, to a $\approx$1-mm^2 spot size, corresponding to a peak power density of $\approx$1 MW/mm^2. The second harmonic in the reflected beam was isolated from the fundamental frequency by a filter and monochromator. Photons at the second harmonic frequency were detected by a photomultiplier tube and counted for 1 or 10 s for 1064- or 532-nm incident light, respectively. A PDP-11 computer controlled the potentiostat (PAR Model 273) and accumulated current measurements and SHG signal.

Results and Discussion

Following insertion of a freshly polished electrode into the electrolyte and subsequent reduction of the air-formed oxide, second harmonic intensity and current were measured as a function of applied potential.

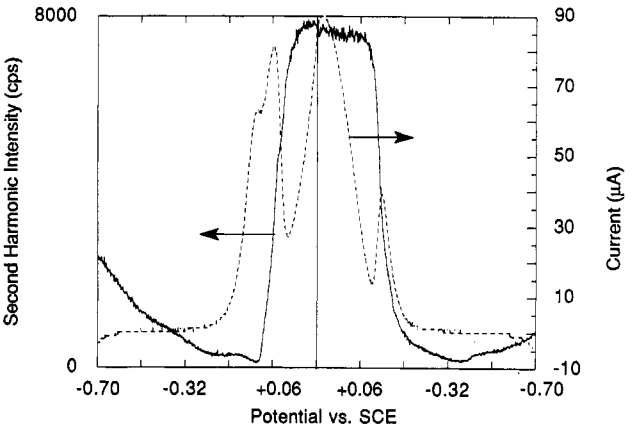

Figure 1. Cyclic voltammogram (CV, broken line) and second harmonic intensity (solid line) from polycrystalline nickel. Incident wavelength is 1064 nm. Sweep rate is 2 mV/s. Data accumulation rate (SHG) = 1 s/data point.

Electrochemistry. A typical first-cycle CV is displayed in Figure 1 (broken line). Note the presence of two partially resolved peaks in the region of $Ni^0 \rightarrow Ni^{2+}$ oxidation (-0.01 to $+0.05$ V_{SCE}) in the anodic half of the CV, followed by a broad feature indicating the onset of pitting–corrosion near the switching potential ($+0.25$ V_{SCE}). Only one peak appears in the cathodic half of the CV ($-0.04V_{SCE}$), yet the sign and position of this current wave indicate oxidation of bare nickel metal.

The presence of two partially resolved current waves in the anodic half of the CV demonstrates that passivation in this electrolyte is a two-step process. An *anodic* current wave in the *cathodic* half of the CV indicates oxidation of *fully reduced nickel metal.* This suggests that the passive film, which forms in the anodic half, is very easily destroyed and is probably very thin. If, after the first cycle, the potential was swept to ≈ -1 V_{SCE} to ensure removal of residual oxide, a very small, broad cathodic wave was observed at ≈ -0.95 V_{SCE}.

Since there is still considerable controversy as to the origin of the two peaks in the $Ni^0 \rightarrow Ni^{2+}$ oxidation region, we will attempt to summarize here some of the previous observations and outline the precautions against contamination that were used in our experiments. Several researchers have observed two peaks in the CV in this potential region;[12,26,27] they concluded that the first peak is due to film formation. At slightly higher voltages, a second type of film forms, resulting in a second peak in the CV. It was later speculated that the presence of the two peaks indicates contamination by an impurity,[28] although the evidence provided did not seem conclusive. In an attempt to address this concern, a number of precautions were undertaken. Extreme care was taken to avoid contamination of the cell and solutions: the quartz cell was regularly soaked in hot nitric acid (50%) and degreased with boiling isopropyl alcohol. In addition, nanopure water was used for rinsing all equipment and as solvent for the electrolyte; the measured resistivity of this water was typically 17.9 MΩ·cm. The sodium chloride and hydrochloric acid, both Fisher products, were certified ACS grade and reagent grade, respectively.

Since many earlier studies have been performed at significantly higher scan rtes, an attempt was made to measure the effect of scan rate on the resolution of the two

(21) Lee, C. H.; Chang, R. K.; Bloembergen, N. *Phys. Rev. Lett.* **1967**, *18*, 167.
(22) Corn, R. M.; Romagnoli, M.; Levenson, M. D.; Philpott, M. R. *J. Chem. Phys.* **1984**, *81*, 4127.
(23) Corn, R. M.; Romagnoli, M.; Levenson, M. D.; Philpott, M. R. *Chem. Phys. Lett.* **1984**, *106*, 30.
(24) Biwer, B. M.; Pellin, M. J.; Schauer, M. W.; Gruen, D. M. *Surf. Sci.* **1986**, *176*, 377.
(25) Boyd, G. T.; Rasing, Th.; Leite, J. R. R.; Shen, Y. R. *Phys. Rev. B* **1984**, *30*, 519.
(26) Weininger, J. L.; Breiter, M. W. *J. Electrochem. Soc.* **1963**, *110*, 484.
(27) Kolotyrkin, Y. M. *Zasch. Met.* **1967**, *3*, 131.
(28) MacDougall, B.; Cohen, M. *J. Electrochem. Soc.* **1975**, *122*, 383.

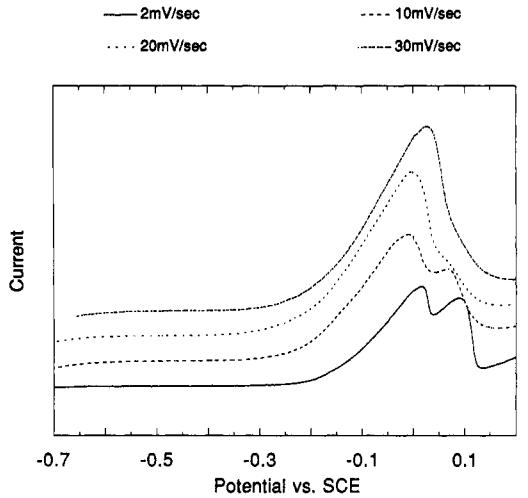

Figure 2. Cyclic voltammograms of polycrystalline nickel at various potential scan rates. Only the half-cycle when the applied potential is increasing is shown. The maximum current is 396, 505, 659, or 741 μA for 2, 10, 20, or 30 mV/s, respectively; in all scans, base-line current is virtually zero.

peaks. Figure 2 shows four CVs run at different scan rates. In each case, the surface was freshly polished and fresh electrolyte was used. Note that an increase in scan rate to only 20 mV/s results in complete blending of the two peaks. All CVs described herein were therefore scanned at 2 mV/s.

Finally, it must be emphasized that the electrochemistry is extremely dependent on electrolyte composition; therefore, it is difficult to make comparisons with earlier studies in different electrolytes. One notes, for example, in comparing the CV of Figure 1 and that of Figure 2 (2 mV/s), that the two peaks are shifted roughly 30 mV higher in the latter figure. Day-to-day variations in solution composition and especially variations in the quality of the polished surface can lead to small potential shifts. In any case, what has *not* varied is the behavior of the second harmonic intensity *concurrent* with the observed peaks in the CV, described below.

Summarizing then, we are confident that the two peaks observed in the present work are not due to contaminants or other spurious effects.

SHG: λ_0 = 1064 nm. The solid line in Figure 1 shows the potential dependence of the observed second harmonic intensity for an incident wavelength of 1064 nm. Note the dramatic increase in intensity that occurs when the second peak of the pair appears in the anodic scan (+0.05 V_{SCE}) and the subsequent drop on the cathodic swing simultaneous with the occurrence of the single peak (−0.04 V_{SCE}) in the CV. The sharp rise in SHG intensity concurrent with the *second* peak in the anodic half of the cycle appears to support a dissolution–precipitation-type mechanism: presumably dissolution of the nickel (the first peak in the CV) would not change the electrical properties of the metal (although it would obviously cause some roughening of the surface). Precipitation (the second peak in the CV), on the other hand, could yield a surface film with an electron structure very different from that of the substrate, and the dramatic change in intensity at this wavelength is suggestive of this. The fact that the SHG does not change until the *second* peak in the CV indicates that actual film formation does not occur until then. The sharp increase in SHG concurrent with film formation suggests that there is an electronic transition in the passive film resonant with either the incident or second harmonic light.[19,20]

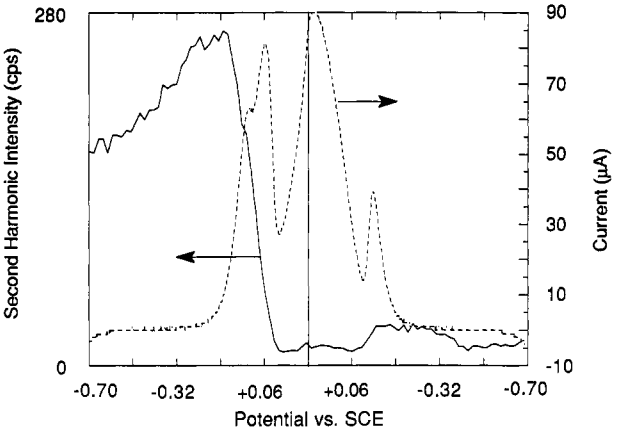

Figure 3. Cyclic voltammogram (CV, broken line) and second harmonic intensity (solid line) from polycrystalline nickel. Incident wavelength is 532 nm. Sweep rate is 2 mV/s. Data accumulation rate (SHG) = 10 s/data point.

As can be seen, the second harmonic intensity remains constant through the pitting–corrosion potential until reactivation of the electrode occurs on the cathodic half of the CV. Pitting–corrosion occurs in such a way that very small holes are created in the film, and hence current due to metal dissolution increases. On the other hand, since the incident laser samples a large region (relative to the pit size), the second harmonic intensity is unchanged.

At passivating potentials, there is an equilibrium between *film* dissolution into the electrolyte and film formation. During the cathodic half of the CV, i.e., the second half of the cycle when the applied potential is decreasing, the potential eventually becomes two low to drive the latter, the film dissolves completely and the second harmonic intensity drops. The metal surface simultaneously is reactivated, and an *anodic* peak occurs. At even lower potentials there is no longer a sufficient driving force for dissolution or film formation; consequently, both current and second harmonic intensity are low.

SHG: λ_0 = 532 nm. The broken line trace in Figure 3 shows a typical CV whereas the solid line shows the second harmonic intensity generated with incident light of 532-nm wavelength. Note that the peak second harmonic intensity is much less than that observed in Figure 1, even when one takes into consideration the difference in incident laser power. In addition, the overall dependence on potential is quite different: second harmonic intensity slowly increases as the potential increases and then drops with the onset of nickel dissolution (−0.01 V_{SCE}). There is a small increase in intensity shortly thereafter (at the pitting–corrosion potential) and again in the cathodic half of the cycle, which appears to occur simultaneously with the single current peak (−0.04 V_{SCE}). The intensity never returns to its initial value at the beginning of the scan, although the anodic switching potential was maintained low enough to avoid serious degradation of surface quality.

The potential dependence of the second harmonic intensity in the case of 532-nm incident light is remarkably different from that observed with incident light of 1064-nm wavelength. The second harmonic intensity at the former wavelength appears to be strongly dependent on surface roughening. The initial intensity slowly drops with the onset of nickel dissolution in the anodic half of the CV. On successive cycling of the electrode, the maximum SHG intensity (observed at ~−1.10 V_{SCE} in the anodic half of the CV) decreases by roughly a factor of 2 for each successive scan. Such a large degradation in signal is not

observed for incident light at the longer wavelength. Scattering is inversely proportional to the fourth power of the wavelength,[29] therefore, scattering due to surface roughening would be an order of magnitude greater at the shorter wavelength. Apparently, at 1064-nm incident light, enhancement of the SHG due to resonance effects more than compensates for any losses due to scattering.

The small subsequent increases in second harmonic intensity can perhaps also be explained by surface roughening. Boyd and co-workers[25] measured SHG from a variety of metals that had been evaporated onto a roughened glass slide and compared this "surface-enhanced" second harmonic intensity with that from the smooth metal. They found that for nickel, a 20-fold increase in absolute second harmonic intensity could be expected for an incident wavelength of 1064 nm. Since local field enhancement (which is the predominant mechanism for this effect) varies linearly with wavelength,[25] one would anticipate a 10-fold enhancement in SHG for an incident wavelength of 532 nm. It should, however, be noted that the roughened substrate they prepared for their measurements was optimal for surface enhancement; the degree of roughening in this experiment is not controlled; hence, one would not expect to observe such a large effect.

Summary and Conclusions

SHG, originating at the interface of a nickel electrode in an acidic chloride solution, has been measured. With incident light at a wavelength of 1064 or 532 nm, striking changes in SHG intensity have been observed with the onset of passive film formation. Analyses of the SHG and electrochemical measurements lead us to a number of conclusions.

Passive film formation on polycrystalline nickel in this electrolyte (0.1 M NaCl, 0.01 m HCl) is a two-step process, as is apparent by the existence of two peaks in the CV. Given the precautions taken to ensure cleanliness, we conclude that the appearance of two peaks at the $Ni^{-} \rightarrow Ni^{2+}$ oxidation potential is not due to impurities in the solution.

The dramatic change in SHG (λ_0 = 1064 nm) concurrent with the second (more anodic) peak in the CV indicates that actual film formation does not occur until the second of the two peaks. This is consistent with a dissolution–precipitation mechanism for film growth on nickel in this electrolyte, as was originally proposed by Reddy and coworkers.[1-3] SHG intensity for an incident wavelength of 532 nm appears to be primarily influenced by surface roughening.

Future work in this area will involve angularly resolved SHG measurements: by rotating a single-crystal electrode about the surface normal and measuring the variation in second harmonic intensity as a function of the angle of rotation, one should be able to determine the crystal symmetry of the film at the interface giving rise to the SHG.[30-37] Such information should be very useful in further elucidating the structure of the passive film on nickel.

Acknowledgment. This work was performed under the auspices of the U.S. Department of Energy, BES-Materials Sciences, under Contract W-31-109-ENG-38.

(29) Born, M.; Wolf, E. *Principles of Optics*; Pergamon Press: New York, 1970.

(30) Tom, H. W. K.; Heinz, T. F.; Shen, Y. R. *Phys. Rev. Lett.* **1983**, *51*, 1983.
(31) Litwin, J. A.; Sipe, J. E.; vanDriel, H. M. *Phys. Rev. B* **1985**, *31*, 5543.
(32) Tom, H. W. K.; Aumiller, G. D. *Phys. Rev. B* **1986**, *33*, 8818.
(33) Shannon, V. L.; Koos, D. A.; Richmond, G. L. *Appl. Opt.* **1987**, *26*, 3579.
(34) Shannon, V. L.; Koos, D. A.; Richmond, G. L. *J. Chem. Phys.* **1987**, *87*, 1440.
(35) Robinson, J. M.; Rojhantalab, H. M.; Shannon, V. L.; Koos, D. A.; Richmond, G. L. *Pure Appl. Chem.* **1987**, *59*, 1263.
(36) Shannon, V. L.; Koos, D. A.; Richmond, G. L. *J. Phys. Chem.* **1987**, *91*, 5548.
(37) Shannon, V. L.; Koos, D. A.; Robinson, J. M.; Richmond, G. L. *Chem. Phys. Lett.* **1987**, *142*, 323.

Homochiral and Heterochiral Polyesters: Polymers Derived from Mandelic Acid

James K. Whitesell* and John A. Pojman

Department of Chemistry, The University of Texas at Austin, Austin, Texas 78712

Received July 24, 1989

The kinetics of polymerization of racemic and optically active mandelic acid were determined under a variety of conditions. The initial rate of monomer consumption in the reaction with racemic mandelic acid was approximately twice that for the single enantiomer for acid-catalyzed reactions in benzene solution. A significant increase in the rate of consumption of monomer was observed in the reaction of optically active mandelic acid coincident with the formation of the cyclic dimer (mandelide). The structure of the dimer formed from a single enantiomer of mandelic acid was determined by single-crystal X-ray analysis. These observations are consistent with a scheme where the rate of chain extension of dimeric and higher species is greater than that for the formation of dimers and where the cyclic dimer is derived from trimeric and higher species and not from the noncyclic dimer.

Introduction

In 1957 Doty reported a fascinating observation on the rates of formation of polypeptides from carbonic anhydride monomers: the rate of polymerization observed for a single enantiomer was approximately 10 times that for the racemate.[1] With simple, second-order kinetics for the combination of a monomer with a growing peptide, the rate would be reduced by at most a factor of 2 under the scenario where each polymer exhibited a high selectivity for addition of a monomer of the same handedness (or the

(1) Lundberg, R. D.; Doty, P. *J. Am. Chem. Soc.* **1957**, *79*, 3961-72.

0897-4756/90/2802-0248$02.50/0